Neuroscience Letters 658 (2017) 67–72

Contents lists available at ScienceDirect

Neuroscience Letters

journal homepage: www.elsevier.com/locate/neulet

Research paper

Cyclosporine-immunosuppression does not affect survival of transplanted skin-derived precursor Schwann cells in the injured rat spinal cord

Zacnicte May[a], Abel Torres-Espín[a], Ana M. Lucas-Osma[a], Nicholas J. Batty[a], Pamela Raposo[a], Keith K. Fenrich[a], Morgan G. Stykel[b], Tobias Führmann[c], Molly Shoichet[c], Jeff Biernaskie[b], Karim Fouad[a,*]

[a] Department of Physical Therapy, Faculty of Rehabilitation Medicine, and Neuroscience and Mental Health Institute, University of Alberta, Edmonton, AB Canada
[b] Department of Comparative Biology and Experimental Medicine, Faculty of Veterinary Medicine, Alberta Children's Hospital Research Institute, University of Calgary, Calgary, AB Canada
[c] Department of Chemical Engineering & Applied Chemistry, Department of Chemistry, Institute of Biomaterials and Biomedical Engineering, University of Toronto, Toronto, ON Canada

ARTICLE INFO

Keywords:
Skin-derived precursor cell
Schwann cell
Spinal cord injury
Immune response

ABSTRACT

A major goal of Schwann cell (SC) transplantation for spinal cord injury (SCI) is to fill the injury site to create a bridge for regenerating axons. However, transplantation of peripheral nerve SCs requires an invasive biopsy, which may result in nerve damage and donor site morbidity. SCs derived from multipotent stem cells found in skin dermis (SKP-SCs) are a promising alternative. Regardless of source, loss of grafted SCs post-grafting is an issue in studies of regeneration, with survival rates ranging from ~1 to 20% after ≥6 weeks in rodent models of SCI. Immune rejection has been implicated in these low survival rates. Therefore, our aim was to explore the role of the immune response on grafted SKP-SC survival in Fischer rats with a spinal hemisection injury. We compared SKP-SC survival 6 weeks post-transplantation in: (I) cyclosporine-immunosuppressed rats (n = 8), (II) immunocompetent rats (n = 9), and (III) rats of a different sub-strain than the SKP-SC donor rats (n = 7). SKP-SC survival was similar in all groups, suggesting immune rejection was not a main factor in SKP-SC loss observed in this study. SKP-SCs were consistently found on laminin expressed at the injury site, indicating detachment-mediated apoptosis (i.e., anoikis) might play a major role in grafted cell loss.

1. Introduction

Promoting axonal regeneration is the focus of many treatment strategies for spinal cord injury (SCI) [1]. One obstacle for axonal growth is created by tissue destruction at the epicenter of the SCI. One strategy to create a bridge for regenerating axons is grafting cells into the injury site. Schwann cells (SCs) are one of the most investigated cell types for grafting post-SCI [2]. The pre-clinical literature on SCI shows that SC grafts can form permissive bridges for axonal regeneration [3], re-myelinate axons [4], and release growth-promoting factors [5]. SCs are typically harvested from nerve biopsies [6,7], but this method may cause patient discomfort and sensory deficits [8]. An alternative source of SCs are multipotent dermal stem cells, which are relatively easy to obtain from skin samples and differentiated into SCs in culture to > 95% purity [9]. Skin-derived precursor SCs (SKP-SCs) have shown promise by promoting axonal growth and re-myelination in rats with SCI [10].

To create a bridge for axonal growth, high numbers of grafted cells must survive within the SCI site, a major challenge in cell transplantation. Survival rates of SCs for example 6–9 weeks post-transplantation range from ~1 to 20% [11–13]. One cause of cell loss post-grafting is immune rejection [14]. Hence, to minimize the risk of rejection in cell transplantation studies, inbred animal strains are preferred over other strains [15]. One of the most investigated inbred rat strains is Fischer (F344), accounting for 32.1% of cases where inbred rat strains are used [16]. Different suppliers sell Fischer rats and the same supplier may carry more than one Fischer rat sub-strain. For example, Charles River carries two Fischer sub-strains SAS™ and CDF™ that share the same MHC haplotype $RT1^{lv}$ [17]. However, 5854 genomic variants have been identified between Fischer rat sub-strains, which may influence protein function and associated biology [18]. Genomic variance between sub-strain mismatched cell donor and recipient could possibly trigger transplant rejection.

Other factors involved in grafted cell loss include the inflammatory

* Corresponding author at: Faculty of Rehabilitation Medicine, 3-87 Corbett Hall, University of Alberta, Edmonton, AB T6G2G4, Canada.
E-mail address: Karim.Fouad@ualberta.ca (K. Fouad).

http://dx.doi.org/10.1016/j.neulet.2017.08.045
Received 27 June 2017; Received in revised form 1 August 2017; Accepted 17 August 2017
Available online 24 August 2017
0304-3940/

environment of the injured spinal cord [14], disruption of blood vessels causing ischemic necrosis [19] and anoikis [20,21]. Anoikis is apoptosis due to detachment from extracellular matrix (ECM) molecules [20]. The contributions and interactions of immunity, inflammation, devascularization, anoikis and other factors in transplanted cell loss are yet to be determined. Although transplant cell death is often discussed, systematic exploration of the factors leading to grafted cell loss is lacking. Thus, the goal of our study was to explore the involvement of the immune response in SKP-SC loss post-transplantation in Fischer rats with hemisection SCI. We compared SKP-SC survival at the SCI site in sub-strain matched cyclosporine-immunosuppressed rats, sub-strain matched rats, and sub-strain mismatched rats. We hypothesized the greatest survival would be found in sub-strain matched immunosuppressed rats. Our experimental set-up also addressed the question of whether sub-strain mismatching lowers grafted cell survival.

2. Materials and methods

2.1. Animals

Adult female Fischer rats (Charles River) of the sub-strains CDF™ (F344/DuCrl; n = 18) and SAS™ (F344/NCrl; n = 7) were used in this study. CDF™ and SAS™ rats weighed between 154 and 189 g and 153–161 g respectively. Sub-strains were housed separately in groups of 6–7 rats in large (18"x14") cages under a 12:12 h light-dark cycle. Animals were housed in a temperature (~24° C) and humidity (~40%) regulated room and had *ad libitum* access to food and water. The experimental groups were: CDF™ rats (CDF; n = 10), CDF™ rats immunosuppressed with cyclosporine (CDF-C; n = 8), and SAS™ rats (SAS; n = 7). Rats were acclimatized to housing conditions for 1 week before starting the experiment. Protocols were approved by the University of Alberta Health Science Animal Care and Use Committee, and the University of Calgary Animal Care Committee.

2.2. SKP-SCs

SKPs were isolated from adult female Fischer (CDF™) rats and differentiated into SCs as described previously [9]. The single change from the protocol was the regular treatment of cultures with the antibiotic Plasmocin™ (5 μg/ml; Invitrogen). SKP-SCs were transduced with a lentivirus encoding green fluorescent protein (GFP) [22]. After transduction, SKP-SCs were enriched for $p75^+$ and GFP^+ cells using a FACS Aria III cell sorter (BD Biosciences). Our previous studies show that neither lenti infection nor FAC sorting results in diminished SKP-SC viability [9,22].

Cryopreserved GFP^+ SKP-SCs (passage 5) were thawed and re-suspended in SC proliferation medium [9] at a density of 100,000 cells/ml on laminin (4 μg/ml; Fisher Scientific) and poly-D-lysine (20 μg/ml; Fisher Scientific) coated polystyrene 10 cm petri dishes (BD Falcon). Cultures were kept at 37° C with 5% CO_2 and fed SC proliferation medium every 3–4 days until 75% confluence.

2.3. Spinal cord hemi-section injury and SKP-SC transplantation

Rats were anesthetised with isoflurane gas (5% induction; 2–3% maintenance), the back was shaved, and then disinfected with chlorhexidine digluconate (Sigma-Aldrich Canada Ltd.). Tears Naturale lubricant (Alcon Canada, Inc.) was applied to the eyes for protection. Back skin was cut longitudinally and the muscles below were dissected to expose vertebra T8, which was removed by laminectomy. A lateral hemisection of the right half of the spinal cord was made with spring scissors through an opening in the dura. 1% dry agarose (Fisher Scientific) was used to cover the opening. Briefly, 0.5 g of agarose was dissolved in 50 ml of dH2O, boiled while stirring for 10 min, and then just enough solution was poured to cover the surface of 10 cm petri dishes. Petri dishes were left to dry overnight in a sterile fume hood. Muscles were sutured with vycril 5-0 (Johnson & Johnson Medical Pty Ltd.), and skin was closed with 9 mm stainless steel staples (Stoelting Co.). Rats were treated for pain with subcutaneous (SQ) buprenorphine injections (0.03 mg/kg; Temgesic, Schering-Plough) and hydrated with SQ saline injections (2.5 ml).

Infected and FAC sorted SKP-SCs were transplanted 2 weeks post-SCI. SKP-SCs were detached from culture plates by incubating the cells at 37° C with the dissociation enzyme Triple E express (3 ml/10 cm petri dish; Invitrogen) for 5 min. Immediately before transplantation, SKP-SCs were counted on a hemocytometer and mixed with a physical blend of hyaluronic acid and methylcellulose (0.5%/0.5% w/v, HAMC) at a concentration of 50,000 cells/μl as previously described [23]. ~200,000 total cells (4 μl) were injected into the SCI site with a 10 μl Hamilton syringe. The SCI/transplant site was covered with dry agarose. Surgical procedures and post-operative care were identical for the SCI and transplantation surgeries. One CDF™ rat died during surgery. The CDF-C group received daily injections of cyclosporine (SQ, 15 mg/kg; Novartis) diluted in saline (2.5 mg/ml), while the CDF and SAS groups received saline injections starting the day before transplantation until euthanasia.

2.4. Behavioural assessment

Locomotor ability was assessed weekly using the Basso, Bresnahan and Beattie (BBB) rating scale [24] and BBB sub-scale [25] for 8 weeks.

2.5. Perfusion and histology

Rats were euthanized 8 weeks post-SCI with pentobarbital (intraperitoneally, 1000 mg/kg; Euthanyl; Biomeda-MTC) and perfused intra-cardially with heparin (0.02 g/L; Fisher Chemical) containing saline and phosphate-buffered 4% paraformaldehyde/5% sucrose (PFA; 0.1 M; pH 7.4). Spinal cords were removed surgically, post-fixed in PFA overnight at 4° C, and immersed in 30% sucrose for 5 days. Spinal tissue was coated with O.C.T cryoprotectant (Sakura Finetek) before freezing in 2-methylbutane (Fisher Scientific) over dry ice. 1.8 cm segments of spinal cord with the SCI in the middle were cut horizontally at 25 μm on a NX70 cryostat (Fisher Scientific) and staggered across four sets of 2 slides. Slides were stored at −20 °C until histological processing.

Immunohistochemistry: Sections were blocked for 1 h at room temperature (RT) with 10% normal goat serum (NGS; Vector) in TBS with 0.5% Triton X-100 (TBS-TX). Primary antibodies were diluted in 1% NGS in TBS and applied overnight at 4° C: polyclonal chicken (ck) anti-GFP (1:1000; Abcam), monoclonal clone GA5 mouse (ms) anti-glial fibrillary acidic protein (GFAP; 1:700), polyclonal rabbit (rb) anti-ionized calcium-binding adapter molecule 1 (Iba-1; 1:1000; Wako), and polyclonal rabbit (rb) anti-laminin (1:500; Abcam). Secondary antibodies were diluted in 1% NGS in TBS and applied for 2 h at RT: AF555 goat (gt) anti-ms, AF555 gt anti-rb, and AF647 gt anti-ck (1:500; all from Invitrogen). Slides were coverslipped with Fluoromount G (Southern Biotech) and imaged with an upright Leica DM6000 B microscope and a Leica DMi8 confocal microscope (Leica Microsystems Inc.).

DAB stain: Sections were blocked with 0.3% hydrogen peroxide in phosphate-buffered saline (PBS) and 10% NGS in TBS-TX for 1 h at RT. rb anti-GFP (1:500; Invitrogen) was diluted in 1% NGS in TBS and applied to slides overnight at 4° C. The next morning, slides were incubated with biotinylated goat anti-rb IgG (Vectastain Elite ABC HRP kit, Vector Laboratories) in 1% NGS in TBS for 2 h at RT. Slides were then incubated with avidin/biotinylated horseradish peroxidase solution for 2 h at RT and reacted with 3,3′-diaminobenzidine (DAB) stain solution (DAB peroxidase HRP reaction kit; Vector Laboratories Inc.) for 30 s. Lastly, sections were immersed in 0.5% cresyl violet for 2 min, and rinsed in dH2O. Tissue was serially dehydrated, cleared in xylene, and coverslipped with Permount^R (Fisher Scientific). Slides were imaged

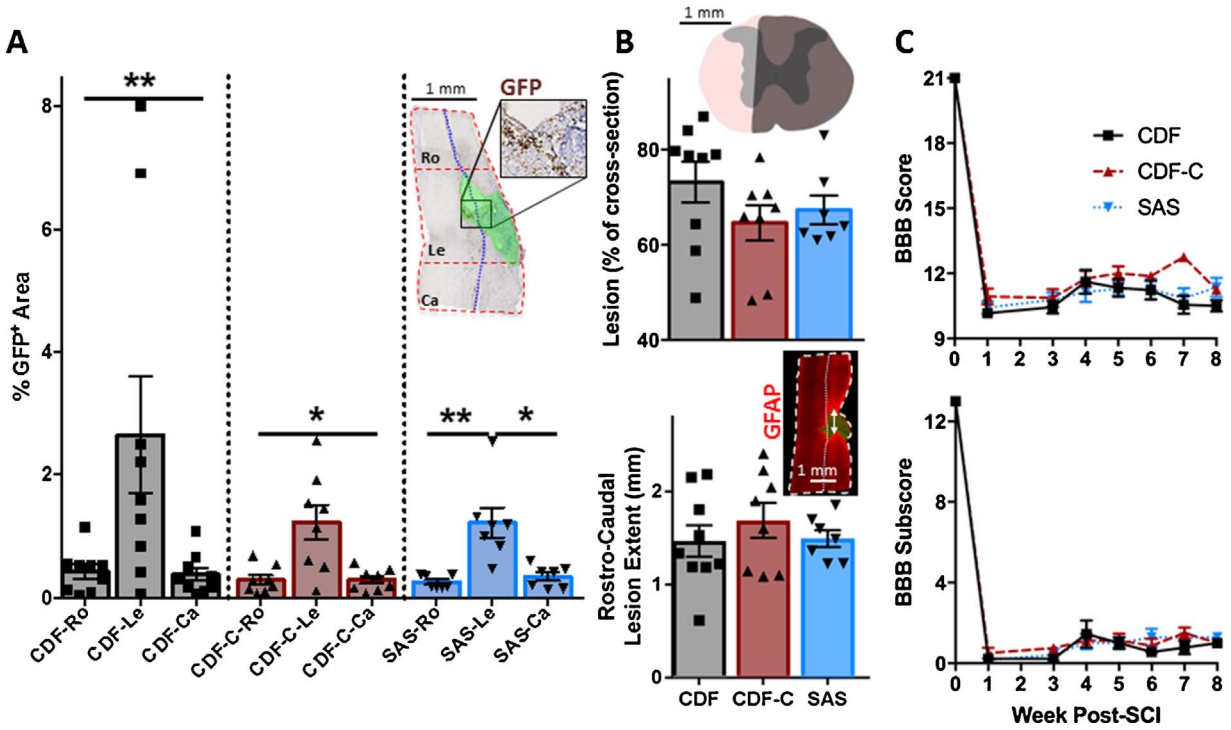

Fig. 1. SKP-SC survival, spinal tissue damage, and locomotor ability were similar between immunosuppressed (CDF-C), immunocompetent (CDF), and sub-strain mismatched rats (SAS). (A) Bars show the average area (% of total area) covered by SKP-SCs at different areas of interest: level of the spinal lesion (Le), and rostral (Ro) and caudal (Ca) to the lesion. Inset images, red dashed lines mark each area of interest on a representative horizontal spinal cord section stained with cresyl violet (purple) and DAB (dark brown). Dotted blue line, midline. Green shaded area, lesion. (B, top) Bars show the lesion area (% cross-section). Representative cross-section schematic of spinal cord. Dark grey shaded area, lesion. (B, bottom) Bars show the rostro-caudal extension (mm) of the lesion. Representative horizontal spinal cord section stained for GFAP (red). White dashed lines mark the section borders. Dotted white line, midline. Green shaded area, lesion. Double-headed arrow, lesion length. Symbols on (A) and (B) bar graphs represent individual rat data. (C) Symbols on graphs represent average weekly BBB scale and sub-scale scores. $p < 0.05$*, $p < 0.01$**. (For interpretation of the references to colour in this figure legend, the reader is referred to the web version of this article.)

with a Leica DMLB light microscope (Leica Microsystems Inc.).

2.6. SKP-SC survival and lesion analysis

SKP-SC survival: The area of GFP$^+$ cells stained with DAB at the SCI and rostral and caudal to the SCI (up to 2.5 mm from the injury) was measured. Overview images of five sections ~275 µm apart were taken with a 5x (0.15 NA) objective lens. Images were analyzed using ImageJ v.1.43 (National Institutes of Health). The area of interest (AOI: SCI, rostral or caudal) was selected and a threshold applied to highlight the DAB signal. The DAB labelled areas at the SCI, rostral, and caudal divisions were averaged across sections and standardized to the total AOI.

Cross-sectional lesion size: One set of slides with sections 75 µm apart extending from the dorsal to ventral surfaces of the spinal cord was analyzed under phase-contrast microscopy. The SCI was identified by the disruption of linear organization of white matter tracts and loss of darkly appearing soma in the grey matter. Maximum lesions were reconstructed by hand on T9 (overlayed by T8) cross-section schematics obtained from the Atlas of the Rat Spinal Cord [26]. The SCI area was calculated as a percentage of the total cross-sectional area.

Rostro-caudal lesion extent: Overview images of GFAP-stained sections (n = 5 sections) ~275 µm apart were taken with a 5x (0.15 NA) objective lens and the distance [µm] between the rostral and caudal SCI borders was measured on ImageJ 1.43 µ and the average plotted.

2.7. SKP-SC morphology and possible association with phagocytic immune cells

To determine the health status of grafted SKP-SCs, morphological analysis was conducted. The criterion for a "healthy" SKP-SC was a bipolar shape with a central cell body and an extension on either end, as seen after differentiation of SKPs to a mature SC phenotype [9,10]. The criterion for an "unhealthy" SKP-SC was a round morphology with one or zero extensions, based on morphological findings of dying SCs [27,28]. Additionally, the presence or absence of Iba-1$^+$ microglia/macrophages immediately adjacent to SKP-SCs was recorded. Every section 75 µm apart on one set of slides was inspected with a 10x (0.3 NA) objective lens to locate GFP$^+$-positive SKP-SCs. Sections containing GFP$^+$-positive SKP-SCs were imaged with a 20x (0.5 NA) objective lens to determine morphology and possible association with phagocytes.

2.8. SKP-SC apposition with laminin

GFP$^+$-positive SKP-SCs were located by inspecting sections 75 µm apart on one slide set with a 10x (0.3 NA) objective lens on an epifluorescence microscope. Then, appositions between laminin-positive staining and GFP$^+$-positive SKP-SCs were assessed with a 20x (0.5 NA) objective lens under epifluorescence. To confirm there was no space between laminin and SKP-SCs, appositions were assessed with a 63x (0.17 NA) oil-immersion lens on a confocal microscope. Appositions were considered true when GFP$^+$-positive SKP-SCs contacted laminin in the same z-plane of confocal z-stacks. Z-step size was 0.76 µm.

2.9. Statistical analysis

All results were analyzed with GraphPad Prism 7 (GraphPad Software Inc.). Data were assessed for normality using the Shapiro-Wilk test. Between-group comparisons (i.e., SKP-SC survival and lesion analysis) were made with one-way ANOVA followed by Brown Forsythe's post-hoc test for parametric data or Kruskal-Wallis followed by Dunn's post-hoc test for non-parametric data. Between-group comparisons of weekly BBB scores and sub-scores were made with two-way ANOVA followed by Tukey's post-hoc test. Within-group comparisons (i.e., SKP-SC survival at the SCI level, and rostral and caudal to the SCI)

were conducted with repeated measures one-way ANOVA followed by Tukey's post-hoc test or with the non-parametric equivalent Friedman's test with Dunn's post-hoc test. Data are shown as mean ± SEM with $p < 0.05$.

3. Results

3.1. SKP-SC survival, spinal tissue damage, and locomotor recovery were unaffected by immune suppression or sub-strain mismatching

SKP-SC survival: Surviving cells were found in all groups, but no significant differences between groups were found at the injury site ($p = 0.64$), rostral to the injury ($p = 0.72$), or caudal to it ($p = 0.77$; Fig. 1A). However, within-group comparisons showed a significant difference in GFP^+ area between the injury site, above and below injury ($p < 0.05$). GFP^+ area was greatest at the injury site compared to above and below the injury, irrespective of treatment group ($p < 0.05$; Fig. 1A). Two conclusions can be drawn from these data. First, SKP-SCs tend to stay within the site of SCI, which shows SKP-SCs may be useful for bridging the injury for growing axons. Second, survival is unaffected by immunosuppression or sub-strain mismatching, suggesting immune rejection is not a major factor in SKP-SC post-transplantation loss in this study.

Lesion cross-sectional size and rostro-caudal extent: No significant differences in% cross-sectional damage ($p = 0.27$) or rostro-caudal extension of damage ($p = 0.58$; Fig. 1B) were found between groups. In sum, neither immune suppression nor sub-strain mismatching in combination with cell grafts influenced the amount of spinal cord tissue damage.

Locomotor recovery: The BBB locomotor rating scale and BBB subscale were used to assess locomotor recovery of rats after SCI and SKP-SC transplantation. No significant group effect was found over the course of 8 weeks post-SCI; 6 weeks post-transplantation ($p = 0.14$; Fig. 1C). Similarly, no group effect was found ($p = 0.74$; Fig. 1C). These results show that neither immunosuppression nor sub-strain mismatching impacted locomotor recovery of graft-recipient rats post-SCI.

3.2. SKP-SCs showed different morphologies and appeared to contact phagocytic immune cells

To assess the status of grafted SKP-SCs, cell morphological analysis was performed. Three SKP-SC morphologies were identified: (I) bipolar-shape (Fig. 2Aa), (II) unipolar or small round cells (Fig. 2Ab), and (III) large brightly fluorescent round cells (Fig. 2Ac). (I) SKP-SCs were considered "healthy", while (II, III) were considered "unhealthy". The three morphologies were found in all the experimental groups. Bipolar and unipolar SKP-SCs appeared to contact microglia/macrophages (Fig. 2Aa & Ab) and brightly fluorescent round cells were surrounded by macrophages/microglia (Fig. 2Ac). In conclusion, SKP-SC morphology varied, with some cells showing characteristics of healthy SCs and others showing characteristics of unhealthy SCs. Further, microglia/macrophages were found close to SKP-SCs.

3.3. SKP-SCs formed appositions with laminin

Since surviving SKP-SCs were located at the level of the SCI, we tested whether these regions contained laminin, a growth substrate for SKP-SCs [29]. We found that SKP-SCs were located in regions with dense laminin staining. Further inspection showed that all SKP-SCs examined formed close appositions with laminin (i.e., there was no discernible gap between SKP-SC soma or processes and laminin staining; Fig. 2B). This result suggests that attachment to substrata is important for SKP-SC survival post-transplantation.

4. Discussion

SCs are often transplanted to fill the SCI site, bridging the injury for axonal regeneration [2]. However, low survival of grafted SCs in the injured spinal cord presents a continuing problem [10–13]. Immune rejection has been shown to contribute to grafted cell loss [14], which is why inbred rat strains are used in transplantation studies (i.e., syngeneic grafting). Despite this, many questions regarding immune rejection remain unanswered, such as the impact of donor and host sub-strain mismatching and the contribution of different factors to grafted cell loss. Addressing these questions is important for the development of approaches to increase survival rates. Here, we investigated the effect of minimizing the immune response and sub-strain mismatching on grafted SC survival. We grafted SKP-SCs into the injured rat spinal cord, since SKP-SCs have been proposed as a more accessible alternative to nerve-derived SCs [9]. SKP-SCs are differentiated from dermal stem/progenitors found in skin [9], rather than nerve biopsies that may result in further damage [8]. Cyclosporine-immunosuppressed Fischer rats were chosen for the transplantation, because this strain of rats is one of the most common inbred rat strains [16], making the present work applicable to a wide audience. Also, we did not consider it justifiable to use a more severe model of immunodeficiency (e.g., nude rats) for a proof of principle study. Here we have shown that pharmacological immunosuppression using cyclosporine does not impact grafted cell survival in one rat strain. Further studies may be of interest employing more severe models of immunodeficiency.

Locomotor function post-transplantation of SKP-SCS into the SCI site was comparable between immunosuppressed, immunocompetent, and sub-strain mismatched Fischer rats. This is consistent with findings that SC transplantation for bridging a SCI often requires adjunct therapy to promote locomotor recovery [7,30]. However, it should be considered that the BBB score was the only measure of locomotor recovery in our study, and it is possible more sensitive methodologies (e.g., kinematics) would have detected group differences in recovery. Similarity of locomotor function between groups in the first week post-SCI (before SKP-SC transplantation) showed the amount of spinal cord tissue damage was likely consistent across groups. This was confirmed in cross-sectional lesion size and rostro-caudal analysis, which were equivalent between groups. Thus, differences in tissue damage from the initial lesions did not confound our results.

SKP-SCs were mainly found at the SCI site, where cells were grafted, with few cells migrating rostral or caudal to the injury. Limited migration of SKP-SCs makes them useful for bridging the SCI and supporting axonal growth, because SKP-SCs can fill the injury gap, providing a substrate for axons extending across the gap. Immune suppression did not increase SKP-SC survival relative to immunocompetent and sub-strain mismatched rats. This finding does not imply that immune rejection is uninvolved in SKP-SC loss. SKP-SCs were found in close proximity to Iba-1^+ immune cells and adopted a round morphology associated with dying SCs [27,28]. Large spherical SKP-SCs appeared to be undergoing necrotic swelling [31]. It should be noted, however, the presence of Iba-1^+ cells could have been related to the injury itself, transplantation vehicle, or dry agarose covering the transplantation site, rather than a response to grafted cells.

Cyclosporine does not suppress all aspects of the immune system and its pharmacokinetics are highly variable [32]. For example, cyclosporine inhibits T and B lymphocytes, some antigen-presenting cells, mast cells, eosinophils, and natural killer cells [33]. However, macrophage activity, including phagocytosis, reactive oxygen species production, and MHC gene expression, is largely unaffected by cyclosporine [33]. Therefore, macrophage activity may have precipitated SKP-SC death and clearance. In future studies, to more fully elucidate the roles of specific immune cell types on SKP-SC death, different immunosuppressive drugs with different pharmacokinetics and mechanisms of action could be tested. For example, FK605 (Tracolimus) is 10–100 times more potent than cyclosporine at lymphocyte inhibition

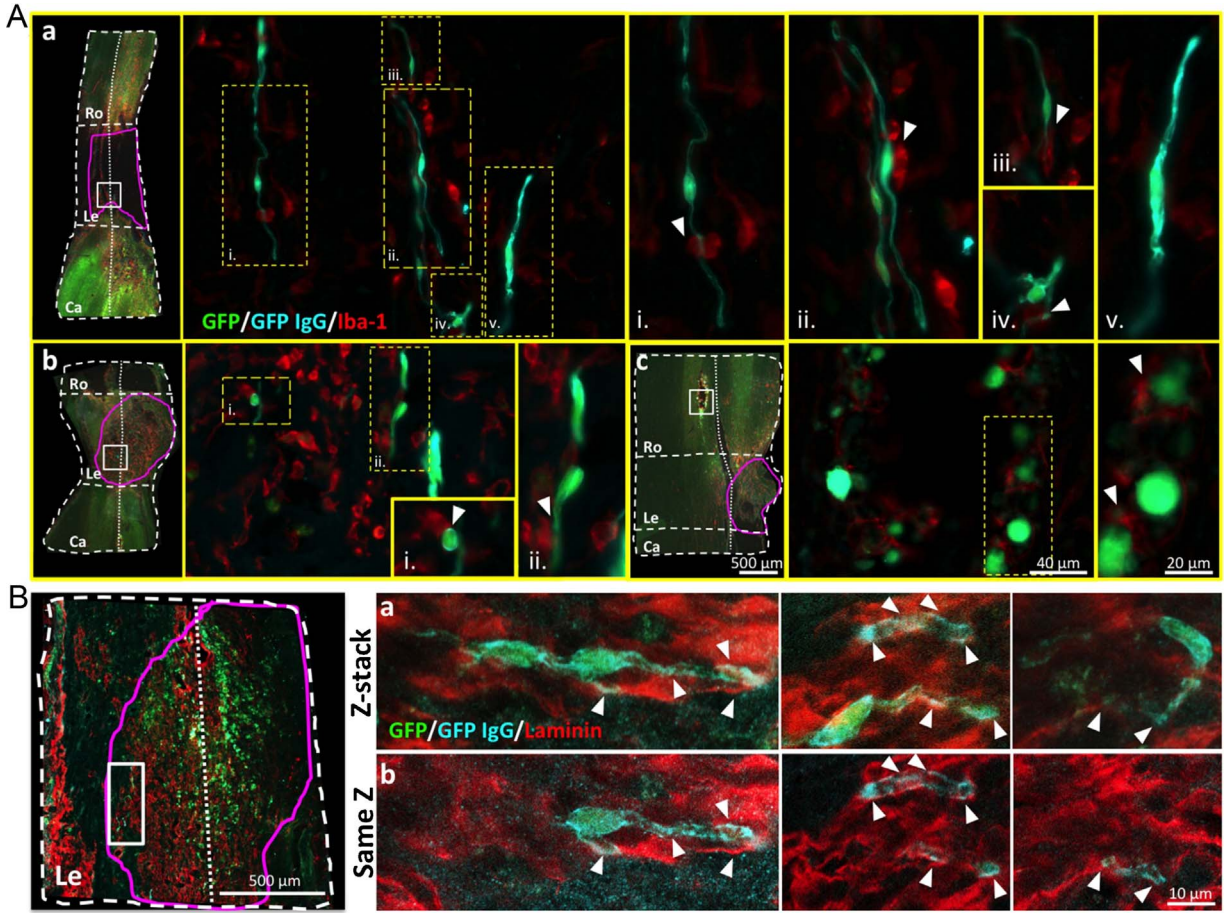

Fig. 2. SKP-SCs showed different morphologies and attached to laminin. (A). SKP-SCs (green/cyan) with varied morphologies showed proximity with Iba-1$^+$ immune cells (red). White dashed lines mark areas of interest (Le: Lesion, Ro: Rostral, and Ca: Caudal) on horizontal spinal cord sections. Dotted white line, midline. Magenta line, lesion borders. White box, location SKP-SCs magnified in adjacent pictures. a. SKP-SCs with a central soma and a process on either end of the soma. b. SKP-SCs with either one process or none. c. Large round SKP-SCs surrounded by immune cells. Roman numerals indicate various examples of SKP-SCs. (B). a. SKP-SCs (green/cyan) contact laminin (red) in images averaging a confocal z-stack. b. SKP-SCs contact laminin on the same z-plane. (For interpretation of the references to colour in this figure legend, the reader is referred to the web version of this article.)

[34] and suppresses the function of activated macrophages [35], which would shed light on the role of macrophages in SKP-SC death.

Different inflammatory consequences of various SCI models could influence grafted cell survival. For example, the model used in the present work was a thoracic hemisection. Peripheral macrophage infiltration is substantial after transection compared to contusion SCI (as the meninges are cut), resulting in exacerbation of secondary degeneration [36]. Exacerbated degeneration could promote grafted cell loss, making it difficult to detect the pro-survival effects of immunosuppressive treatments. In another example, it has been found that immune function is disrupted more after cervical than thoracic SCI, suggesting that immunosuppression might have a stronger effect in cervical models [37]. These findings highlight the need for rigorous preclinical testing of cell transplant viability using a range of SCI models and locations to optimize the potential for successful clinical trials.

Sub-strain mismatching did not decrease SKP-SC survival compared to sub-strain matching. Sub-strain mismatched Fischer rats might be too genetically invariant and not elicit a strong enough immune response to lower survival below that seen with sub-strain matching. Nevertheless, our results suggest that the immune response is not the most important factor in grafted cell loss. To investigate another factor influencing grafted cell survival, we assessed the apposition between SKP-SCs and laminin, since laminin is an important ECM molecule involved in cell attachment [29]. Laminin is strongly expressed at the site of CNS trauma [38]. SKP-SC morphology, as a measure of health, was assessed separately from SKP-SC laminin appositions. However, surviving SKP-SCs were consistently found in close proximity to laminin at the site of injury. Hence, it is likely that both healthy and unhealthy SKP-SCs interacted with laminin. Nevertheless, the finding of SKP-SC appositions with laminin agrees with the idea that anoikis, apoptosis resulting from substrate detachment [20], is possibly a key factor in grafted cell survival. In fact, inhibiting the Laminin y1 gene in SCs results in depletion of all laminin isoforms expressed by SCs and increases rates of SC apoptosis/caspase signalling [39]. Further, plating SCs on non-adherent substrates leads to SC death [21], and transplantation of SCs in hydrogel vehicles with laminin promotes SC survival in the injured rat spinal cord compared to media vehicle [40]. Future experiments grafting SCs in the same vehicle with and without attachment molecules in the injured spinal cord will be necessary to establish a causal relation between detachment and SC post-transplantation loss. Another factor likely contributing to grafted SC death is vascular disruption in SCI, leading to ischemic necrosis [19]. Therefore, the role of vascularization in SC transplant survival should be carefully explored.

Grafted SC survival in SCI is frequently discussed but poorly understood. Immune rejection is thought to be a main factor contributing to low grafted cell survival [14]. In our SCI model we show that the immune system is likely not a main factor involved in SKP-SC survival. Understanding the factors regulating grafted cell survival will permit us to maximize survival within the SCI site, bridging the injury for regenerating axons in pre-clinical models.

Acknowledgements

This study was supported by a CIHR operating grant (RES0011338, KF). Morgan G. Stykel was supported by a Queen Elizabeth II Graduate Scholarship.

References

[1] M.H. Tuszynski, O. Steward, Concepts and methods for the study of axonal regeneration in the CNS, Neuron 74 (5) (2012) 777–791, http://dx.doi.org/10.1016/j.neuron.2012.05.006.
[2] W. Tetzlaff, E.B. Okon, S. Karimi-Abdolrezaee, C.E. Hill, J.S. Sparling, J.R. Plemel, et al., A systematic review of cellular transplantation therapies for spinal cord injury, J. Neurotrauma 28 (8) (2011) 1611–1682, http://dx.doi.org/10.1089/neu.2009.1177.
[3] R.R. Williams, M. Henao, D.D. Pearse, M.B. Bunge, Permissive Schwann cell graft/spinal cord interfaces for axon regeneration, Cell Transplant. 24 (1) (2015) 115–131, http://dx.doi.org/10.3727/096368913X674657.
[4] J.S. Sparling, F. Bretzner, J. Biernaskie, P. Assinck, Y. Jiang, H. Arisato, et al., Schwann cells generated from neonatal skin-derived precursors or neonatal peripheral nerve improve functional recovery after acute transplantation into the partially injured cervical spinal cord of the rat, J. Neurosci. 35 (17) (2015) 6714–6730, http://dx.doi.org/10.1523/JNEUROSCI. 1070-14.2015.
[5] C. Meier, E. Parmantier, A. Brennan, R. Mirsky, K.R. Jessen, Developing Schwann cells acquire the ability to survive without axons by establishing an autocrine circuit involving insulin-like growth factor, neurotrophin-3, and platelet-derived growth factor-BB, J. Neurosci. 19 (10) (1999) 3847–3859.
[6] R.P. Bunge, Changing uses of nerve tissue culture 1950–1975, The Nervous System Volume 1. The Basic Neuroscience Raven Press, New York, 1975.
[7] K. Fouad, L. Schnell, M.B. Bunge, M.E. Schwab, T. Liebscher, D.D. Pearse, Combining Schwann cell bridges and olfactory-ensheathing glia grafts with chondroitinase promotes locomotor recovery after complete transection of the spinal cord, J. Neurosci. 25 (5) (2005) 1169–1178, http://dx.doi.org/10.1523/JNEUROSCI.3562-04.2005.
[8] D.A. Hilton, J. Jacob, L. Househam, C. Tengah, Complications following sural and peroneal nerve biopsies, J. Neurol. Neurosurg. Psychiatry 78 (11) (2007) 1271–1272, http://dx.doi.org/10.1136/jnnp.2007.116368.
[9] J.A. Biernaskie, I.A. McKenzie, J.G. Toma, F.D. Miller, Isolation of skin-derived precursors (SKPs) and differentiation and enrichment of their Schwann cell progeny, Nat. Protoc. 1 (6) (2007) 2803–2812, http://dx.doi.org/10.1038/nprot.2006.422.
[10] J. Biernaskie, J.S. Sparling, J. Liu, C.P. Shannon, J.R. Plemel, Y. Xie, et al., Skin-derived precursors generate myelinating Schwann cells that promote remyelination and functional recovery after contusion spinal cord injury, J. Neurosci. 27 (36) (2007) 9545–9559, http://dx.doi.org/10.1523/JNEUROSCI.1930-07.2007.
[11] M. Enomoto, M.B. Bunge, P. Tsoulfas, A multifunctional neurotrophin with reduced affinity to p75NTR enhances transplanted Schwann cell survival and axon growth after spinal cord injury, Exp. Neurol. 248 (2013) 170–182, http://dx.doi.org/10.1016/j.expneurol.2013.06.013.
[12] K.L. Golden, D.D. Pearse, B. Blits, M.S. Garg, M. Oudega, P.M. Wood, M.B. Bunge, Transduced Schwann cells promote axon growth and myelination after spinal cord injury, Exp. Neurol. 207 (2) (2007) 203–217, http://dx.doi.org/10.1016/j.expneurol.2007.06.023.
[13] D.D. Pearse, A.R. Sanchez, F.C. Pereira, C.M. Andrade, R. Puzis, Y. Pressman, et al., Transplantation of Schwann cells and/or olfactory ensheathing glia into the contused spinal cord: survival, migration, axon association, and functional recovery, Glia 55 (9) (2007) 976–1000, http://dx.doi.org/10.1002/glia.20490.
[14] C.E. Hill, L.D.F. Moon, P.M. Wood, M.B. Bunge, Labeled Schwann cell transplantation: cell loss, host Schwann cell replacement, and strategies to enhance survival, Glia 53 (3) (2006) 338–343, http://dx.doi.org/10.1002/glia.20287.
[15] T. Kurosawa, Inbred animal strains, in: John Wiley & Sons, Ltd (Ed.), Encyclopedia of Life Sciences, John Wiley & Sons, Ltd, Chichester, UK, 2009, , http://dx.doi.org/10.1002/9780470015902.a0001442.pub2.
[16] M.F.W. Festing, Rat Strains, (2006) (Retrieved from http://isogenic.info/html/rat_strains.html).
[17] Charles River Laboratories, Inbred Rats Datasheet, (2015) (Retrieved from http://www.criver.com/files/pdfs/rms/inbred-rats.aspx).
[18] R. Hermsen, J. de Ligt, W. Spee, F. Blokzijl, S. Sch'fer, E. Adami, et al., Genomic landscape of rat strain and substrain variation, BMC Genomics 16 (1) (2015), http://dx.doi.org/10.1186/s12864-015-1594-1.
[19] J.D. Balentine, Pathology of experimental spinal cord trauma. I. The necrotic lesion as a function of vascular injury, Lab. Invest. 39 (3) (1978) 236–253.
[20] S.M. Frisch, Disruption of epithelial cell-matrix interactions induces apoptosis, J. Cell Biol. 124 (4) (1994) 619–626, http://dx.doi.org/10.1083/jcb.124.4.619.
[21] M. Koda, Y. Someya, Y. Nishio, R. Kadota, C. Mannoji, T. Miyashita, et al., Brain-derived neurotrophic factor suppresses anoikis-induced death of Schwann cells, Neurosci. Lett. 444 (2) (2008) 143–147, http://dx.doi.org/10.1016/j.neulet.2008.07.055.
[22] W. Rahmani, S. Abbasi, A. Hagner, E. Raharjo, R. Kumar, A. Hotta, et al., Hair follicle dermal stem cells regenerate the dermal sheath, repopulate the dermal papilla, and modulate hair type, Dev. Cell 31 (5) (2014) 543–558, http://dx.doi.org/10.1016/j.devcel.2014.10.022.
[23] T. Führmann, R.Y. Tam, B. Ballarin, B. Coles, I. Elliott Donaghue, D. van der Kooy, et al., Injectable hydrogel promotes early survival of induced pluripotent stem cell-derived oligodendrocytes and attenuates longterm teratoma formation in a spinal cord injury model, Biomaterials 83 (2016) 23–36, http://dx.doi.org/10.1016/j.biomaterials.2015.12.032.
[24] D.M. Basso, M.S. Beattie, J.C. Bresnahan, Graded histological and locomotor outcomes after spinal cord contusion using the NYU weight-drop device versus transection, Exp. Neurol. 139 (2) (1996) 244–256, http://dx.doi.org/10.1006/exnr.1996.0098.
[25] P.G. Popovich, C.A. Tovar, P. Wei, L. Fisher, L.B. Jakeman, D.M. Basso, A reassessment of a classic neuroprotective combination therapy for spinal cord injured rats: LPS/pregnenolone/indomethacin, Exp. Neurol. 233 (2) (2012) 677–685, http://dx.doi.org/10.1016/j.expneurol.2011.11.045.
[26] C. Watson, G. Paxinos, G. Kayalioglu, C. Heise, Atlas of the rat spinal cord, The Spinal Cord, Elsevier, 2009, pp. 238–306, http://dx.doi.org/10.1016/B978-0-12-374247-6.50019-5.
[27] J. Nakao, J. Shinoda, Y. Nakai, S. Murase, K. Uyemura, Apoptosis regulates the number of Schwann cells at the premyelinating stage, J. Neurochem. 68 (5) (1997) 1853–1862.
[28] D.E. Syroid, P.R. Maycox, P.G. Burrola, N. Liu, D. Wen, K.F. Lee, et al., Cell death in the Schwann cell lineage and its regulation by neuregulin, Proc. Natl. Acad. Sci. U. S. A. 93 (17) (1996) 9229–9234.
[29] K. Tohyama, C. Ide, The localization of laminin and fibronectin on the schwann cell basal lamina, Arch. Histol. Cytol. 47 (5) (1984) 519–532, http://dx.doi.org/10.1679/aohc.47.519.
[30] D.D. Pearse, F.C. Pereira, A.E. Marcillo, M.L. Bates, Y.A. Berrocal, M.T. Filbin, M.B. Bunge, cAMP and Schwann cells promote axonal growth and functional recovery after spinal cord injury, Nat. Med. 10 (6) (2004) 610–616, http://dx.doi.org/10.1038/nm1056.
[31] S. Elmore, Apoptosis: a review of programmed cell death, Toxicol. Pathol. 35 (4) (2007) 495–516, http://dx.doi.org/10.1080/01926230701320337.
[32] A.W. Thomson, The effects of cyclosporin A on non-T cell components of the immune system, J. Autoimmun. 5 (Suppl A) (1992) 167–176.
[33] D.J. Reynolds, J.K. Aronson, ABC of monitoring drug therapy. Cyclosporin. BMJ, Br. Med. J. 305 (6867) (1992) 1491–1494.
[34] D.H. Peters, A. Fitton, G.L. Plosker, D. Faulds, Tacrolimus. A review of its pharmacology, and therapeutic potential in hepatic and renal transplantation, Drugs 46 (4) (1993) 746–794.
[35] T. Yoshino, H. Nakase, Y. Honzawa, K. Matsumura, S. Yamamoto, Y. Takeda, et al., Immunosuppressive effects of tacrolimus on macrophages ameliorate experimental colitis, Inflamm. Bowel Dis. 16 (12) (2010) 2022–2033, http://dx.doi.org/10.1002/ibd.21318.
[36] P.G. Popovich, Z. Guan, P. Wei, I. Huitinga, N. van Rooijen, B.T. Stokes, Depletion of hematogenous macrophages promotes partial hindlimb recovery and neuroanatomical repair after experimental spinal cord injury, Exp. Neurol. 158 (2) (1999) 351–365, http://dx.doi.org/10.1006/exnr.1999.7118.
[37] W.F. Kliesch, J.M. Cruse, R.E. Lewis, G.R. Bishop, B. Brackin, Restoration of depressed immune function in spinal cord injury patients receiving rehabilitation therapy, Paraplegia 34 (2) (1996) 82–90.
[38] F. Hu, S.M. Strittmatter, The N-terminal domain of nogo-a inhibits cell adhesion and axonal outgrowth by an integrin-specific mechanism, J. Neurosci. 28 (5) (2008) 1262–1269, http://dx.doi.org/10.1523/jneurosci.1068-07.2008.
[39] W.-M. Yu, M.L. Feltri, L. Wrabetz, S. Strickland, Z.-L. Chen, Schwann cell-specific ablation of laminin 1 causes apoptosis and prevents proliferation, J. Neurosci. 25 (18) (2005) 4463–4472, http://dx.doi.org/10.1523/JNEUROSCI.5032-04.2005.
[40] V. Patel, G. Joseph, A. Patel, S. Patel, D. Bustin, D. Mawson, et al., Suspension matrices for improved schwann-cell survival after implantation into the injured rat spinal cord, J. Neurotrauma 27 (5) (2010) 789–801, http://dx.doi.org/10.1089/neu.2008.0809.